An artificial intelligence system reveals liquiritin inhibits SARS-CoV-2 by mimicking type I interferon

Jie Zhu[1*], Yong-Qiang Deng[2*], Xin Wang[1*], Xiao-Feng Li[2*], Na-Na Zhang[2], Zurui Liu[3], Bowen Zhang[1], Cheng-Feng Qin[2,#], Zhengwei Xie[1,#]

[1]Peking University International Cancer Institute and Department of Pharmacology, School of Basic Medical Sciences, Peking University, Beijing, China
[2]State Key Laboratory of Pathogen and Biosecurity, Beijing Institute of Microbiology and Epidemiology, Academy of Military Medical Sciences, Beijing, China
[3]Gigaceuticals Co. Ltd., Beijing, China

*These authors contributed equally

Correspondence:
Zhengwei Xie: xiezhengwei@hsc.pku.edu.cn
Chengfeng Qin: qincf@bmi.ac.cn

Abstract

The pandemic COVID-19 has spread to all over the world and greatly threatens safety and health of people. COVID-19 is highly infectious and with high mortality rate. As no effective antiviral treatment is currently available, new drugs are urgently needed. We employed transcriptional analysis to uncover potential antiviral drugs from natural products or FDA approved drugs. We found liquiritin significantly inhibit replication of SARS-CoV-2 in Vero E6 cells with EC_{50} = 2.39 μM. Mechanistically, we found liquiritin exerts anti-viral function by mimicking type I interferon. Upregulated genes induced by liquiritin are enriched in GO categories including type I interferon signaling pathway, negative regulation of viral genome replication and etc. In toxicity experiment, no death was observed when treated at dose of 300 mg/kg for a week in ICR mice. All the organ indexes but liver and serum biochemical indexes were normal after treatment. Liquiritin is abundant in licorice tablet (~0.2% by mass), a traditional Chinese medicine. Together, we recommend liquiritin as a competitive candidate for treating COVID-19. We also expect liquiritin to have a broad and potent antiviral function to other viral pathogens, like HBV, HIV and etc.

Introduction

Began at the end of year 2019, a novel coronavirus named SARS-CoV-2 caused outbreaks of pulmonary diseases (COVID-19) worldwide. It has greatly threatened the public health in global and killed tens-of-thousands of people[1]. By May 2nd, there are > 340,000 cumulative cases globally, with > 240,000 deaths. At present, some drugs are considered

modestly effective in treating COVID-19, including chloroquine and remdesivir. However, the efficacy and safety of these drugs for SARS-CoV-2 pneumonia patients are not conclusive after several clinical trials. Current studies showed controversial effects in different trials[2]. As there is no specific treatment against COVID-19, identifying effective and safe antiviral agents to combat the disease is urgently needed.

Previous strategies for anti-viral drug development mainly focus on blocking receptors or inhibiting proteases. However, boosting the protective ability of the host was rarely considered. Herein, we consider a method to inhibit the gene expression of multiple factors that related to viral replication with one single compound. Previously, the chemical treated cell cultures were measured and analyzed by microarray or L1000 techniques[3,4]. The gene set enrichment analysis (GSEA) or Venn diagram were applied to connect the gene expression profile to up / down gene sets of certain diseases. Such technique, named connectivity map (CMAP) has been applied in screening drugs for obesity[5,6]. We proposed that similar strategy can be applied to inhibit host machinery proteins that supporting the viral replication and to induce genes that blocking the viral replication.

Liquiritin is one of the main flavonoids in *Glycyrrhiza uralensis*, which acts as an antioxidant and has antidepressant, neuroprotective, anti-inflammatory and therapeutic effects on heart system diseases[7-11]. Liquiritin plays a strong protective effect on vascular endothelial cells in myocardial ischemia-reperfusion injury model[11]. It can also protect smoking-induced lung epithelial cell injury[12].

Type I interferon (INF) is important cytokines to protect host from viral infection. Almost all human cells can produce INFα/β, which are the best-defined type I INFs. INFs are able to induce the downstream IFN stimulated genes (ISGs) to inhibit the viral replication, including MX1, PKR, OAS, IFITM, APOBEC1, TRIM and etc[13].

In present study, we first predicted the efficacy of compounds to inhibit the viral replication. Then, we tested them using Vero E6 cell lines. We found liquiritin is able to inhibit infection of SARS-CoV-2 efficiently with EC_{50} = 2.39 μM. Mechanistically, we found liquiritin mimicked type I INF to induce ISGs and thus protect cells from infection. We also evaluated the bioavailability, metabolism and safety of liquiritin.

Results

Prediction of efficacy against host genes related to viral replication

To perform GSEA against chemical induced transcriptomes, a gene set is required. In the case of SARS-CoV-2, a reasonable gene set that are enriched in viral processes by analyzing the ACE2-expressed AT2 cells were reported by Zhao et. al[14]. These genes include TRIM27, IFITM3, TMPRSS2, LAMP1 and etc. The full list is shown in Methods section. We chose the FDA approved drugs and natural products as the compound library (3682 in total). We employed InfinityPhenotype[15], which is an artificial intelligence based platform, to predict

efficacy of potential drugs (Figure 1a). InfinityPhenotype takes molecule formula as input and calculate the enrichment score, similar as in CMAP, but only one side is considered. All the scores were plotted in Figure 1b. The top scored compounds are shown in Supp. Table 1. In the natural product list, liquiritin (-0.32) and agnuside (-0.31) have emerged. In FDA approved drugs, we obtained procaterol (-0.23), pibrentasvir (-0.23) and carbocisteine (-0.21). Liquiritin ranks first among all the compounds.

In Vitro verification of the efficacy

To experimentally verify the predicted results, we measured the effects of these compounds on the virus yield and infection rates of SARS-CoV-2. First, a cytopathic effect (CPE) inhibition assay with only one dose was performed in Vero E6 cells (ATCC-1586) for fast screening. Among the five tested drugs, liquiritin exhibited significant CPE inhibition at 10 μM qualitatively. We then employed qRT-PCR to quantify the inhibition and expanded the concentration from 0.1 to 100 μM. Vero E6 cells were infected with SARS-CoV-2 at 100 μl median tissue culture infectious dose ($TCID_{50}$). Notably, liquiritin potently blocked virus infection at low-micromolar concentration (EC_{50} = 2.39 μM, Figure 1c).

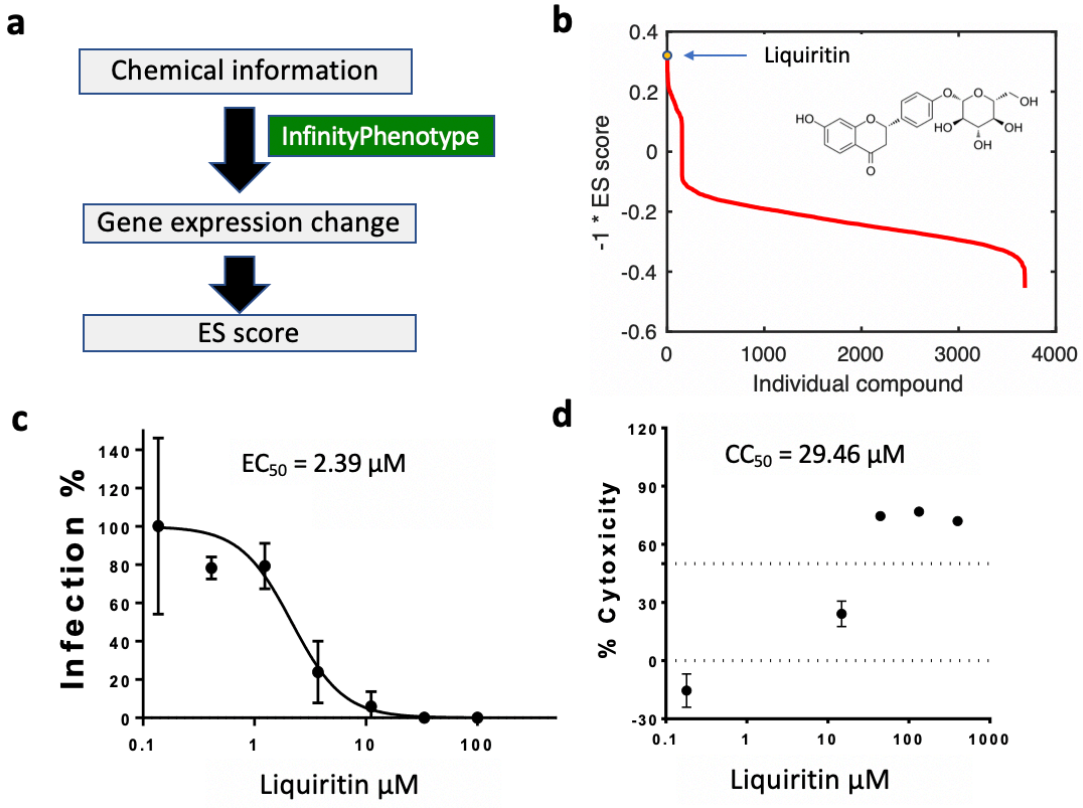

Figure 1 The antiviral activities of the liquiritin against SARS-CoV-2 *in vitro*.
a) The workflow of the computation of enrichment score (ES). b) The ES score of all compounds. Liquiritin ranks first. c) The antiviral activity of liquiritin in Vero E6 cells (EC_{50} = 2.39 μM, n = 3 for where error bar is shown). d) Cytotoxicity of the liquiritin to Vero E6 cells was measured by MTS assay.

Transcriptomic analysis of cell line treated with liquiritin

The transcriptomic change induced by liquiritin (Figure 2a) in MCF7 cells was reported by Li et al[4]. Gene Ontology analysis reveals that the upregulated genes are enriched in the "type I interferon signaling pathway", "negative regulation of viral genome replication", "defense response to virus" and "response to virus" categories (Figure 2b) with *p*-value < 8.26e-4, 8.29e-4, 0.0021 and 0.0039, respectively. Nine genes in the first category were IFIT1, IFIT3, IFITM1, IFI6, IFI27, OAS3, OAS1, PSMB8 and IRF8. The induced ISGs include MX1, OAS, IFIT, IFITM and etc. as shown in the "negative regulation of viral genome replication" category. IFIT1 and IFIT3 belong to the type I interferon (IFN)-induced protein with tetratricopeptide repeats (IFIT) family and IFITM1 belongs to the IFN-induced transmembrane protein (IFITM) family. Thus, liquiritin exhibits a general anti-viral activity by mimicking the type I IFN. Further, the enrichment analysis of protein-protein interaction networks reveals a significant module composed of nine ISGs (Figure 2d). Other genes in this module indicate potential regulators of these ISGs.

Further, the "inflammatory response" is also enriched in down-regulated genes with *p*-value < 0.015 (Figure 2c), showing liquiritin reduced inflammatory response. In this category, IL13, IL17B and etc. showed up. This may be beneficial for avoiding the cytokine storm observed in COVID-19.

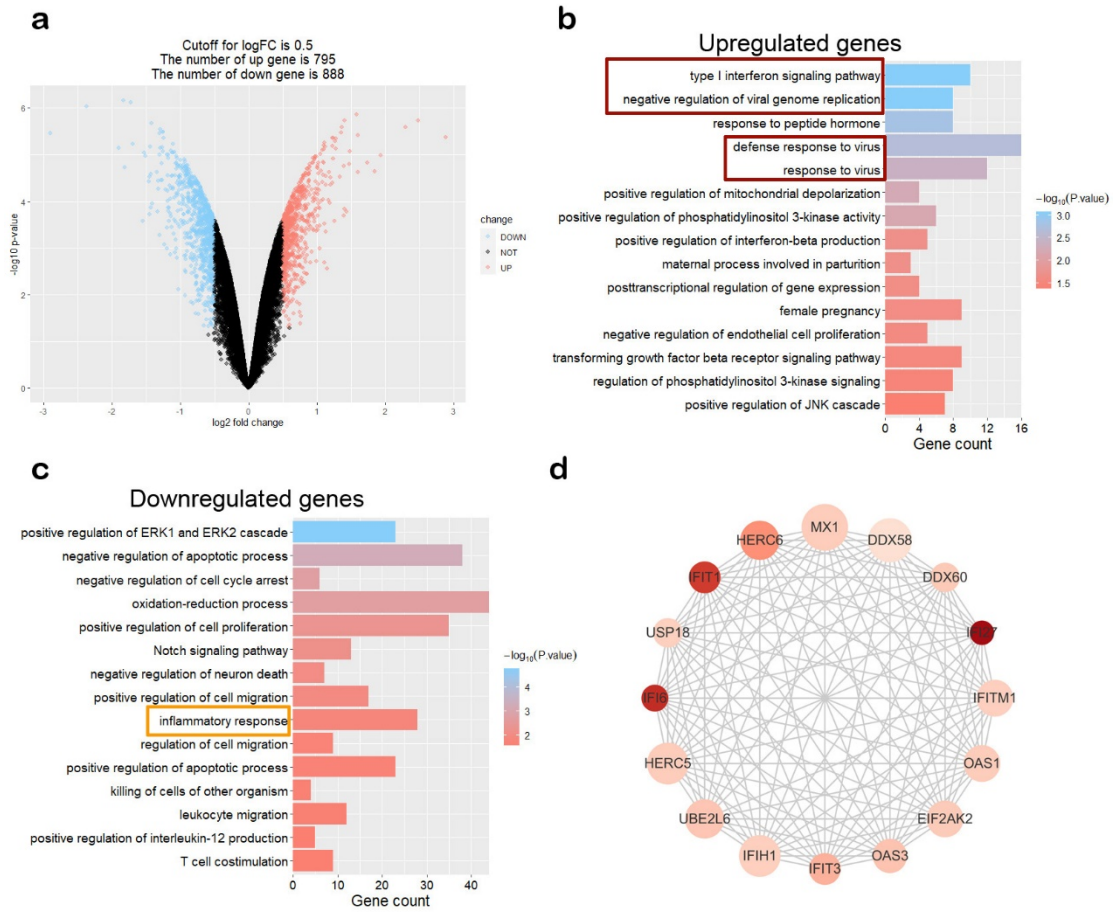

Figure 2 Transcriptomic analysis of cell line treated with liquiritin.
a) Volcano plot of the differentially expressed genes (DEGs) in MCF7 cells treated with liquiritin compared to that in normal cells. Gene Ontology analysis of upregulated genes (b) and that of downregulated genes (c). d) The most significant module of the protein-protein interaction (PPI) network of upregulated genes. Node size is positively related to degree of genes and the gradation of color positively associated with the expression change of this gene.

Liquiritin does not inhibit 3CL^{pro}

Liu et al.[18] found derivatives of flavones efficiently inhibit 3CL^{pro}, which is a conserved protease for SARS-CoV-2 replication. Liquiritin is also a derivative of flavones, specifically it is a monosaccharide derivative and a monohydroxyflavanone. It has a mother nucleus structure similar to the compounds found by Liu et al. Though molecule docking showed there might be a binding to 3CL^{pro}, liquiritin didn't show any inhibitory effects to the activity of 3CL^{pro} *in vitro* at 12.5, 25.0 and 50.0 μM (data not shown).

Liquiritin is a safe candidate for treating COVID-19

To evaluate the safety of liquiritin, the cytotoxicity in Vero E6 cells was determined by MTS assay (CC_{50} = 29.46 μM, Maximal inhibition of cell growth is 70%, as shown in Figure 1d). We further examined the toxicity in vivo. No morality was observed at 150 mg/kg dose of one-time treatment of liquiritin by intravenous administration during the 14 days monitoring period (Figure 3a). Mice intravenous administration 150 mg/kg of liquiritin did not manifest any signs of toxicity during this observation period. The body weight, food intake and water intake are shown in Figure 3b, c. A continuous treatment for seven days at 300 mg/kg was also performed. The mortality rate is also zero (Figure 3d). The intake food, body weights were all kept at normal level (Figure 3e, f). As reported in literatures, liquiritin has no significantly cytotoxic effects in L-02, GES-1, IMR-90 and 293T cells with different concentrations (30, 60, 90, 120, and 150 μM) and the MTT assay results confirmed that 345 μM liquiritin has no influence on the viability of RA-FLS cells[16,17].

For both assays shown in Figure 3a, d, we also measured organ and serum biochemical indexes. No significant differences organ indexes (ratio of organ weight to body weight) were observed except liver index compared with the control mice. Meanwhile, levels of glucose, cholesterol, triglyceride, high-density lipoprotein (HDL-C), and low-density lipoprotein (LDL-C) kept normal after liquiritin administration. We observed declined ALT and it may be due to the anti-inflammatory effect of liquiritin. Meanwhile, no abnormality was observed in levels of blood UREA、UA、CK、α-HBDH, suggesting renal function and heart function were not harmed. Though some relevant index of blood analysis, such as the number of leukocytes, neutrophils and etc., in the control mice and liquiritin-treated mice are different, they are all within the range of reference values, indicating that liquiritin has no obvious toxicity (Supplementary Table 6-9).

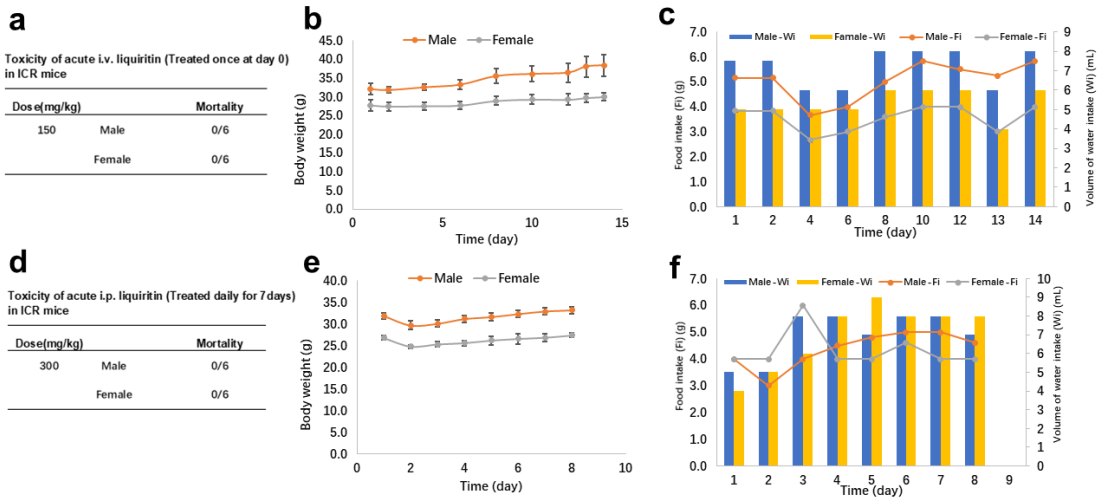

Figure 3 The Toxicity assay for liquiritin in ICR mice.

a) Mortality rate of acute i.v. liquiritin in ICR mice. b, c) Body weight, food intake and water intake at 150 mg/kg dose of one-time treatment of liquiritin by intravenous administration during the 14 days monitoring period in ICR mice. d) Mortality rate of acute i.p. liquiritin in ICR mice. e, f) Body weight, food intake and water intake at 300 mg/kg dose of liquiritin by i.p. administration for seven days in ICR mice.

Pharmacokinetics survey of liquiritin

To evaluate the pharmacokinetics of liquiritin, we searched literatures and found the pharmacokinetic data of mixtures containing liquiritin (Supp. Table 2). The corresponding dose of liquiritin is range from 225 to 44, 000 ug/kg, the C_{max} in serum is range from 0.064 to 2.3 μM. The T_{max} is range from 0. 25 to 0. 6 hours and $T_{1/2}$ is range from 1.9 to 11.63 hours. As the bioavailability is low and degradation is fast, we suggest an intravenous or inhalation administration for liquirtin.

Discussion

To find drugs that may cure COVID-19, we adopted a different strategy by analyzing transcriptional changes induced by various compounds. We found that liquiritin is highly effective in the inhibition of SARS-CoV-2 infection *in vitro* compared to other SARS-CoV-2 drugs reported *in vitro* (Supp. Table 3). Since liquiritin is also one of the main ingredients of compound licorice tablets, we speculate that it is safe. Indeed, it didn't show toxicity and side effects in two independent experiments. In summary, we suggest that liquiritin should be assessed in human patients suffering from the COVID-19.

Mechanistically, we found liquiritin induced the expression of anti-viral genes. GO analysis revealed that "type I INF signaling pathway" was activated. We thus proposed that liquiritin may mimic type I INF to inhibit the viral replication. Vero E6 cell line we used here lack IFNB1 gene and cannot synthesize interferon. However, Vero E6 cells contain the *trans*-acting factors needed for human beta interferon[20]. It's still responsive to

human INF. Thus, liquiritin acted through downstream of INF synthesis.

We also surveyed the literatures for the targets of liquiritin. It's reported that liquiritin, a flavonoid isolated from Glycyrrhiza, is a potent and competitive AKR1C1 inhibitor with IC_{50} of 0.62 μM, 0.61 μM, and 3.72μM for AKR1C1, AKR1C2 and AKR1C3, respectively[19]. Whether AKR1 is the major target for liquiritin's anti-viral activity is unclear. Further experiments need to be carried out.

So far, there are no first principles to precisely simulate the intrinsic interactions of cells. One alternative solution is to use the measured data to overcome the difficulty of complex systems. Deep neural network offers an option to empirically fit high dimensional data. InfinityPhenotype we employed here is based on transcriptional change induced by compounds. Such framework treated a broad range of interactions inside the cells, from ligand-protein interaction to transcriptional regulations, as well as other hidden interactions, as a black box. It offers us an opportunity to predict the efficacy of compounds in a precise manner.

To test if other gradients in liquorice inhibit the viral replication, we also tested liquiritigenin and glycyrrhizic acid in Vero E6 cells. Neither of them showed inhibitory effect (data not shown). Further animal test, transcriptional measurement with virus in Vero E6 cells and in mice are still ongoing. Because type I interferon is responsive to most viruses that infect vertebrate, we expect liquiritin having a broad and potent antiviral function to other viral pathogens, like HBV, HIV and etc.

Methods

Virus and Cells

The stock of SARS-CoV-2 strain BetaCoV/wuhan/AMMS01/2020 was originally isolated from a patient returning from Wuhan. The virus was amplified and titerated by standard plaque forming assay on Vero cells. All experiments involving infectious SARS-CoV-2 were performed in biosafety level 3 (BSL3) containment laboratory in AMMS. Vero cell were purchased from ATCC (Cat# CCL-81) and cultured in DMEM supplemented with 10% FBS at 37℃.

Prediction of efficacy

The full list of genes used for enrichment analysis (GSEA) includes SLC1A5, CXADR, CAV2, NUP98, CTBP2, GSN, HSPA1B, STOM, RAB1B, HACD3, ITGB6, IST1, NUCKS1, TRIM27, APOE, SMARCB1, UBP1, CHMP1A, NUP160, HSPA8, DAG1, STAU1, ICAM1, CHMP5, DEK, VPS37B, EGFR, CCNK, PPIA, IFITM3, PPIB, TMPRSS2, UBC, LAMP1 and CHMP3. Kolmogorov-Smirnov (KS) test is used to evaluate the distribution of query genes in reference list. The gene expression fold change was calculated by InfinityPhenotype platform and used to make the rank list (>10,000 in this case). The ES score for one gene set

is defined as:

$$\mathrm{ES} = \max_{j=1\ to\ t}\left[\frac{j}{t} - \frac{V(j)}{n}\right]$$

where t is the number of genes in the targeted gene set, n is the number of genes in full gene expression profile, V(j) is the rank of a specific gene in the rank list.

Cytotoxicity assay

The cytotoxicity of the tested drugs on Vero Cell were determined by MTS cell proliferation assays (Promega, USA), according to manufacturer's protocol. Briefly, ~1 × 104 cells were seeded into a 96-well plate and incubated for 20-24 h at 37 °C. The media was removed, and 100 μl of media containing decreasing concentrations of antiviral compound were added to the wells. All determinations were performed in triplicate. After 4 days incubation at 37 °C, MTS assays were performed according to manufacturers' protocols. A microtiter plate reader (SYNERGY HTX, BioTek Instruments) with a 490 nm filter was used to record absorbance. After adjusting the absorbance for background and comparing to untreated controls, the cytotoxic concentration CC50 was calculated using a sigmoidal nonlinear regression function to fit the dose-response curve using the GraphPad Prism 7.0 software.

The in vitro antiviral activity.

The in vitro antiviral efficacy of the tested drug on Vero E6 Cell was performed as we previously described [Jin, et al., 2020]. Briefly, ~1 × 104 cells were seeded into a 96-well plate and incubated for 20-24 h at 37 °C. Cells were pre-treated with the indicated antivirals (10 μM) for 1 h, and the virus (MOI of 0.01) was subsequently added to allow infection for 2 h. Then, the virus-drug mixture was removed and cells were further cultured with fresh drug-containing medium. At 48 h p.i., viral RNA copy in supernatants were quantified by qRT-PCR assays with the SARS-CoV-2-specific primers.

Toxicity study in ICR mice

ICR mice were used to test the in vivo safety of liquiritin. Thirty-Six ICR male and female mice were purchased from the Peking University Animal Department. The animals were housed in a temperature-controlled animal room (24 ± 2 ℃) with a relative humidity of 60-80%. All mice were fasted overnight but given water ad libitum prior to dosage. Animals were divided into two groups with 6 males and 6 females at random. Liquiritin was dissolved in 10% DMSO/40% PEG400/50% Saline and administered i.v. once at doses of 150mg/kg, and administered i.p. once a day for 10 days at doses of 300mg/kg. Their general behavior, signs of toxicity, body weights and mortality were recorded after the administration of liquiritin. Animals were killed by excessive anesthesia. Gross necropsy, weighing, calculation of organ index (brain, heart, lung, liver, kidney, adrenal gland, thymus, spleen, testis, epididymis, ovary, uterus, thyroid), pathological examination of the organs was carried out afterwards. The blood sample was analysis by blood analyzer

HEMAVET 950FS.

Transcriptional analysis

Microarray data on gene expression (GSE85871) was downloaded from Gene Expression Omnibus (GEO). The DEGs between normal and liquirintin-treated MCF7 cells were also screened by the limma package. $|\log2FC| \geq 0.5$, adjust p-value < 0.05 were considered statistically significant for the DEGs. To elucidate potential biological process associated with the DEGs, we performed GO enrichment analysis utilizing the Database for Annotation, Visualization and Integrated Discovery (DAVID). p-value < 0.05 was defined as the cut-off criteria. The upregulated DEGs were mapped to STRING to evaluate the PPI information and set confidence score > 0.4 as the cut-off standard. Cytoscape was used to visualize the PPI network, a practical open–source software tool for the visual exploration of biomolecule interaction networks consisting of protein, gene and other types of interaction.

Enzyme Inhibition Assay

A colorimetric substrate Thr-Ser-Ala-Val-Leu-Gln-pNA (GL Biochemistry Ltd) and assay buffer (40 mM PBS, 100 mM NaCl, 1 mM EDTA, 0.1% Triton 100, pH 7.3) was used for the inhibition assay. Stock solutions of the inhibitor were prepared with 100% DMSO. The 100 μl reaction systems in assay buffer contain 0.5 μM protease and 5% DMSO or inhibitor to the final concentration. First, dilute SARS-CoV-2 3CLpro with assay buffer to the desired concentration. 5 μl DMSO or inhibitor at various concentrations was pre-incubated with 85 μl diluted SARS-CoV-2 3CLpro for 30 min at room temperature. And then add 10 μl 2 mM substrate Thr-Ser-Ala-Val-Leu-Gln-pNA (dissolved in water) into above system to final concentration of 200 μM to initiate the reaction. Increase in absorbance at 390 nm was recorded for 20 min at interval of 30 s with a kinetics mode program using a plate reader (Synergy, Biotek). The percent of inhibition was calculated by V_i/V_0, where V_0 and V_i represent the mean reaction rate of the enzyme incubated with DMSO or compounds. IC50 was fitted with Hill function.

Author Contributions: All authors contributed to the work presented in this paper. J. Z. & W. K. performed the statistical analysis, Z. L. and Z. X performed the efficacy prediction, Y. D., X. L, and N. Z measured the anti-viral activity and performed the analysis. B. Z. performed docking, J. Z. performed the literature review. Z. X & J. Z. wrote the paper. Z. X & C. Q. supervised the team.

Acknowledgement: We thank Hongbo Liu and Luhai Lai for the help of $3CL^{pro}$ assay. Z.W.X was supported by National key research and development program of China (2018YFA0900200), National Natural Science Foundation of China Grants (31771519) and Beijing Natural Science Foundation (5182012). C.F.Q. was supported by the National Science Fund for Distinguished Young Scholar (No. 81925025), and the Innovative Research Group (No. 81621005) from the NSFC, and the Innovation Fund for Medical Sciences (No.2019-I2M-5-049) from the Chinese Academy of Medical Sciences.

REFERENCES

1. Zhu, N., *et al.* A Novel Coronavirus from Patients with Pneumonia in China, 2019. *N Engl J Med* **382**, 727-733 (2020).
2. Grein, J., *et al.* Compassionate Use of Remdesivir for Patients with Severe Covid-19. *N Engl J Med* (2020).
3. Subramanian, A., *et al.* A Next Generation Connectivity Map: L1000 Platform and the First 1,000,000 Profiles. *Cell* **171**, 1437-1452 e1417 (2017).
4. Lv, C., *et al.* The gene expression profiles in response to 102 traditional Chinese medicine (TCM) components: a general template for research on TCMs. *Sci Rep* **7**, 352 (2017).
5. Liu, J., Lee, J., Salazar Hernandez, M.A., Mazitschek, R. & Ozcan, U. Treatment of obesity with celastrol. *Cell* **161**, 999-1011 (2015).
6. Lee, J., *et al.* Withaferin A is a leptin sensitizer with strong antidiabetic properties in mice. *Nat Med* **22**, 1023-1032 (2016).
7. Whorwood, C.B., Sheppard, M.C. & Stewart, P.M. Licorice inhibits 11 beta-hydroxysteroid dehydrogenase messenger ribonucleic acid levels and potentiates glucocorticoid hormone action. *Endocrinology* **132**, 2287-2292 (1993).
8. Tamir, S., *et al.* Estrogenic and antiproliferative properties of glabridin from licorice in human breast cancer cells. *Cancer Res* **60**, 5704-5709 (2000).
9. Hatano, T., *et al.* Phenolic constituents of licorice. VIII. Structures of glicophenone and glicoisoflavanone, and effects of licorice phenolics on methicillin-resistant Staphylococcus aureus. *Chem Pharm Bull (Tokyo)* **48**, 1286-1292 (2000).
10. Takahashi, T., *et al.* Isoliquiritigenin, a flavonoid from licorice, reduces prostaglandin E2 and nitric oxide, causes apoptosis, and suppresses aberrant crypt foci development. *Cancer Sci* **95**, 448-453 (2004).
11. Sun, Y.X., *et al.* Neuroprotective effect of liquiritin against focal cerebral ischemia/reperfusion in mice via its antioxidant and antiapoptosis properties. *J Asian Nat Prod Res* **12**, 1051-1060 (2010).
12. Guan, Y., *et al.* Protective effects of liquiritin apioside on cigarette smoke-induced lung epithelial cell injury. *Fundam Clin Pharmacol* **26**, 473-483 (2012).
13. McNab, F., Mayer-Barber, K., Sher, A., Wack, A. & O'Garra, A. Type I interferons in infectious disease. *Nat Rev Immunol* **15**, 87-103 (2015).
14. Yu Zhao, Z.Z., Yujia Wang, Yueqing Zhou, Yu Ma, Wei Zuo. Single-cell RNA expression profiling of ACE2, the putative receptor of Wuhan 2019-nCov *bioRxiv preprint* (2020).
15. Xie., e.a. InfinityPhenotype. *To be published*.
16. Zhai, K.F., *et al.* Liquiritin from Glycyrrhiza uralensis Attenuating Rheumatoid Arthritis via Reducing Inflammation, Suppressing Angiogenesis, and Inhibiting MAPK Signaling Pathway. *J Agric Food Chem* **67**, 2856-2864 (2019).
17. Wang, J.R., *et al.* Liquiritin inhibits proliferation and induces apoptosis in HepG2 hepatocellular carcinoma cells via the ROS-mediated MAPK/AKT/NF-kappaB

signaling pathway. *Naunyn Schmiedebergs Arch Pharmacol* (2020).

18. Hongbo Liu, *et.al*. Scutellaria baicalensis extract and baicalein inhibit replication of SARS-CoV-2 and its 3C-like protease in vitro . *bioRxiv preprint* (2020).
19. Zeng, C.*, et al.* Liquiritin, as a Natural Inhibitor of AKR1C1, Could Interfere With the Progesterone Metabolism. *Front Physiol* **10**, 833 (2019).
20. Mosca, J.D. & Pitha, P.M. Transcriptional and posttranscriptional regulation of exogenous human beta interferon gene in simian cells defective in interferon synthesis. *Mol Cell Biol* **6**, 2279-2283 (1986).

Supplementary Table 1 Results of InfinityPhenotype platform screening

ID	Name	Drug Groups	score
T7S0344	Liquiritin	natural product	-0.315809062
T3S1363	Agnuside	natural product	-0.308751956
DB01366	Procaterol	approved; investigational	-0.233934229
DB13878	Pibrentasvir	approved; investigational	-0.2277026
DB04339	Carbocisteine	approved; investigational	-0.212099668

Supplementary Table 2 Pharmacokinetic Data of Mixtures Containing Liquiritin

Animal	Compounds	Liquiritin dose	Route	Pharmacokinetic parameters	Ref
Rat	Glycyrrhizae Radix Extract	3.8mg/kg	oral	Cmax：0.064μM Tmax：0.4h T1/2：3.7h	(1)
Rat	Chaihu-Guizhi decoction	225μg/kg	oral	Cmax：0.5μM Tmax：0.11h T1/2：11.63h	(2)
Rat	Tongmai Yangxin Pill	1.337mg/kg	oral	Cmax：0.475μM Tmax：0.5h T1/2：2.16h	(3)
Rat	ZBPYR extract	6.25mg/kg	oral	Cmax：0.5μM Tmax：0.6h T1/2：7.8h	(4)
Rat	Baoyuan Decoction	240.17/600.425 /1200μg/kg	oral	Cmax：0.077/ 0.1156/0.14μM	(5)
Rat	Si-Ni-San extract	16.76mg/kg	oral	Cmax：2.3μM Tmax：0.5h T1/2：7.25h	(6)
Rat	Longhu Rendan pills	2.07mg/kg	oral	Cmax：0.24μM Tmax：0.3h T1/2：1.9h	(7)
Rat (female)	Ge-Gen Decoction	44.0mg/kg	oral	Cmax：0.41μM Tmax：0.25h T1/2：4.26h	(8)

Supplementary Table 2 REFERENCES

1. Han, Y.J., Kang, B., Yang, E.J., Choi, M.K. & Song, I.S. Simultaneous Determination and Pharmacokinetic Characterization of Glycyrrhizin, Isoliquiritigenin, Liquiritigenin, and Liquiritin in Rat Plasma Following Oral Administration of Glycyrrhizae Radix Extract. *Molecules* **24**(2019).
2. Li, Z., *et al.* Simultaneous quantification of fifteen compounds in rat plasma by LC-MS/MS and its application to a pharmacokinetic study of Chaihu-Guizhi decoction. *J Chromatogr B Analyt Technol Biomed Life Sci* **1105**, 15-25 (2019).
3. Shen, J., *et al.* Development of a HPLC-MS/MS Method to Determine 11 Bioactive Compounds in Tongmai Yangxin Pill and Application to a Pharmacokinetic Study in Rats. *Evid Based Complement Alternat Med* **2018**, 6460393 (2018).

4. Zhang, L., Xu, H. & Zhan, L. Pharmacokinetic Assessments of Liquiritin, Protocatechuic Aldehyde and Rosmarinic Acid in Rat Plasma by UPLC-MS-MS After Administration of ZibuPiyin Recipe. *J Chromatogr Sci* **56**, 139-146 (2018).
5. Lu, Y.Y., *et al.* Pharmacokinetics study of 16 representative components from Baoyuan Decoction in rat plasma by LC-MS/MS with a large-volume direct injection method. *Phytomedicine* **57**, 148-157 (2019).
6. Li, T., *et al.* Simultaneous quantification of paeoniflorin, nobiletin, tangeretin, liquiritigenin, isoliquiritigenin, liquiritin and formononetin from Si-Ni-San extract in rat plasma and tissues by liquid chromatography-tandem mass spectrometry. *Biomed Chromatogr* **27**, 1041-1053 (2013).
7. Wang, T., *et al.* Simultaneous quantification of catechin, epicatechin, liquiritin, isoliquiritin, liquiritigenin, isoliquiritigenin, piperine and glycyrrhetinic acid in rat plasma by HPLC-MS/MS: application to a pharmacokinetic study of Longhu Rendan pills. *Biomed Chromatogr* **30**, 1166-1174 (2016).
8. Yan, Y., *et al.* Simultaneous determination of puerarin, daidzin, daidzein, paeoniflorin, albiflorin, liquiritin and liquiritigenin in rat plasma and its application to a pharmacokinetic study of Ge-Gen Decoction by a liquid chromatography-electrospray ionization-tandem mass spectrometry. *J Pharm Biomed Anal* **95**, 76-84 (2014).

Supplementary Table 3 Against SARS-CoV-2 drugs reported *in vitro* and Liquiritin

Number	Drug	EC50	Ref.
1	Remdesivir	0.77μM	(1)
2	Hydroxychloroquine	0.72μM	(2)
3	Chloroquine	1.13μM	(1)
4	Camostat mesylate	1μM	(3)
5	Nitazoxanide	2.12μM	(1)
6	**Liquiritin**	**2.39μM**	This study
7	Ebselen	4.67 μM	(4)
8	CVL218	5.12μM	(5)
7	Nafamostat	22.5uM	(1)
10	Terifunomide	26.06μM	(6)
11	Favipiravir	61.88uM	(1)
12	Leflunomide	63.56μM	(6)
13	Penciclovir	95.96uM	(1)
14	Ribavirin	109.5uM	(1)

Supplementary Table 3 REFERENCES

1. Wang, M., *et al.* Remdesivir and chloroquine effectively inhibit the recently emerged novel coronavirus (2019-nCoV) in vitro. *Cell Res* **30**, 269-271 (2020).
2. Yao, X., *et al.* In Vitro Antiviral Activity and Projection of Optimized Dosing Design of Hydroxychloroquine for the Treatment of Severe Acute Respiratory Syndrome Coronavirus 2 (SARS-CoV-2). *Clin Infect Dis* (2020).
3. Hoffmann, M., *et al.* SARS-CoV-2 Cell Entry Depends on ACE2 and TMPRSS2 and Is Blocked by a Clinically Proven Protease Inhibitor. *Cell* **181**, 271-280 e278 (2020).

4. Jin, Z.*, et al.* Structure of M(pro) from COVID-19 virus and discovery of its inhibitors. *Nature* (2020).
5. Y.G., *et al*. A data-driven drug repositioning framework discovered a potential therapeutic agent targeting COVID-19. *bioRxiv preprint* (2020).
6. R.X., *et al.* Novel and potent inhibitors targeting DHODH, a rate-limiting enzyme in de novo pyrimidine biosynthesis, are broad-spectrum antiviral against RNA viruses including newly emerged coronavirus SARS-CoV-2 *bioRxiv preprint* (2020).

Supplementary Table 4： GO analysis of upregulated genes

Term	Count	%	PValue
GO:0060337~type I interferon signaling pathway	10	0.009291	8.26E-04
GO:0045071~negative regulation of viral genome replication	8	0.007433	8.29E-04
GO:0043434~response to peptide hormone	8	0.007433	0.001488
GO:0051607~defense response to virus	16	0.014866	0.002137
GO:0009615~response to virus	12	0.011149	0.003902
GO:0051901~positive regulation of mitochondrial depolarization	4	0.003716	0.005847
GO:0043552~positive regulation of phosphatidylinositol 3-kinase activity	6	0.005575	0.006636
GO:0032728~positive regulation of interferon-beta production	5	0.004646	0.020022
GO:0060137~maternal process involved in parturition	3	0.002787	0.020706
GO:0010608~posttranscriptional regulation of gene expression	4	0.003716	0.022911
GO:0007565~female pregnancy	9	0.008362	0.023305
GO:0001937~negative regulation of endothelial cell proliferation	5	0.004646	0.025488
GO:0007179~transforming growth factor beta receptor signaling pathway	9	0.008362	0.027777
GO:0014066~regulation of phosphatidylinositol 3-kinase signaling	8	0.007433	0.032987
GO:0046330~positive regulation of JNK cascade	7	0.006504	0.041505

Supplementary Table 5： GO analysis of downregulated genes

Term	Count	%	PValue
GO:0070374~positive regulation of ERK1 and ERK2 cascade	23	0.019502	1.65E-05
GO:0043066~negative regulation of apoptotic process	38	0.032221	5.22E-04
GO:0071157~negative regulation of cell cycle arrest	6	0.005087	0.001725
GO:0055114~oxidation-reduction process	44	0.037308	0.00186
GO:0008284~positive regulation of cell proliferation	35	0.029677	0.004883
GO:0007219~Notch signaling pathway	13	0.011023	0.006354
GO:1901215~negative regulation of neuron death	7	0.005935	0.009122
GO:0030335~positive regulation of cell migration	17	0.014414	0.010436
GO:0006954~inflammatory response	28	0.023741	0.015459
GO:0030334~regulation of cell migration	9	0.007631	0.019467
GO:0043065~positive regulation of apoptotic process	23	0.019502	0.020164
GO:0031640~killing of cells of other organism	4	0.003392	0.023776
GO:0050900~leukocyte migration	12	0.010175	0.024075
GO:0032735~positive regulation of interleukin-12 production	5	0.00424	0.025538
GO:0031295~T cell costimulation	9	0.007631	0.025874

Supplementary Table 6：Body weight, organ index, blood chemistry and blood analysis in control or liquiritin-treated male mice by intravenous injection.

	Control-male	Liquiritin-male
Body weight, g	36.433±0.669	38.650±1.206
Brain index, %	1.163±0.050	1.228±0.043
Thyroid index, %	0.693±0.009	0.618±0.018
Lungs index, %	0.557±0.037	0.512±0.008
Thymus index, %	0.190±0.040	0.163±0.011
Heart index, %	0.430±0.012	0.412±0.017
Liver index, %	4.413±0.217	3.590±0.102**
Spleen index, %	0.327±0.026	0.235±0.024*
Pancreas index, %	0.630±0.069	0.530±0.023
Kidney index, %	1.393±0.057	1.437±0.044
Testis index, %	0.707±0.020	0.613±0.057
Epididymis index, %	0.173±0.022	0.168±0.008
Stomach index, %	0.723±0.048	0.620±0.018*
Bladder index, %	0.083±0.018	0.078±0.003
ALT U/L	64.067±17.767	59.717±8.245
AST U/L	132.4±48.461	99.734±7.371
GLU-God mmol/L	7.947±0.731	4.757±0.623*
TC mmol/L	3.570±0.217	3.920±0.284
TG mmol/L	1.047±0.217	1.180±2.295
TP g/L	54.700±3.308	56.150±2.295
ALB g/L	27.867±0.578	30.85±0.746*
UA umol/L	158.800±30.175	76.067±9.691*
UREA mmol/L	2.197±0.082	2.098±0.064
CK U/L	464.467±138.376	381.7±37.722
α-HBDH U/L	31.933±9.831	34.2±3.569
HDL-C mmol/L	3.133±0.188	3.178±0.270
LDL-C mmol/L	0.370±0.062	0.460±0.024
LDH U/L	329.433±0.062	343.967±31.700
ALP U/L	3.167±0.584	3.617±0.101
T-Bil umol/L	1.933±0.192	1.938±0.098
Number of leukocytes (*103/UL)	5.067±1.012	4.617±0.283
Number of neutrophils (*103/UL)	1.407±0.234	1.072±0.091
Lymphocyte count (*103/UL)	3.367±0.769	3.245±0.205
Number of monocytes (*103/UL)	0.143±0.027	0.223±0.022
Number of eosinophils (*103/UL)	0.107±0.052	0.055±0.027
Number of basophils (*103/UL)	0.047±0.023	0.022±0.014
Percentage of neutrophils	28.163±1.247	23.215±1.477
Lymphocyte percentage	65.807±1.857	70.335±1.962
Monocyte percentage	3.250±1.063	4.898±0.443
Percentage of eosinophils (%)	1.980±1.094	1.107±0.539
Percentage of basophils (%)	0.807±0.430	0.447±0.286

Number of red blood cells (*106/UL)	7.650±0.229	7.343±0.218
Hemoglobin concentration (g/dl)	111.333±3.180	109.333±3.148
Hematocrit (%)	37.833±1.278	36.767±1.207
Mean corpuscular volume (Fl)	49.467±1.320	50.067±0.956
Mean hemoglobin content (pg)	14.567±0.521	14.900±0.221
Mean hemoglobin concentration (g/L)	287.667±10.868	297.833±4.708
RBC distribution width (%)	14.633±0.433	14.983±0.309
Platelet count (*103/UL)	576.667±101.259	631.667±85.693
Mean platelet volume (FL)	4.933±0.219	4.917±0.087

Data are means ± SEM, control (n=3); liquiritin (n=6); *P< 0.05 compared with control mice.

Supplementary Table 7：Body weight, organ index, blood chemistry and blood analysis in control or liquiritin-treated female mice by intravenous injection.

	Control-female	Liquiritin-female
Body weight, g	28.867±0.581	30.283±0.473
Brain index, %	1.583±0.041	1.520±0.035
Thyroid index, %	0.647±0.034	0.680±0.042
Lungs index, %	0.590±0.050	0.612±0.013
Thymus index, %	0.183±0.022	0.215±0.018
Heart index, %	0.427±0.009	0.428±0.018
Liver index, %	4.393±0.170	3.688±0.054**
Spleen index, %	0.403±0.015	0.363±0.021
Pancreas index, %	0.600±0.036	0.597±0.024
Kidney index, %	1.200±0.055	1.145±0.037
Ovary index, %	0.090±0.010	0.127±0.010
Uterus index, %	0.430±0.075	0.520±0.065
Stomach index, %	0.817±0.048	0.722±0.032
Bladder index, %	0.070±0.000	0.065±0.002
ALT U/L	56.133±5.441	40.400±2.912*
AST U/L	107.4±12.450	118.350±2.949
GLU-God mmol/L	5.873±0.779	5.315±0.772
TC mmol/L	2.65±0.560	2.968±0.166
TG mmol/L	0.617±0.116	0.740±0.080
TP g/L	55.333±3.290	61.083±1.554
ALB g/L	30.600±0.321	34.183±0.715*
UA umol/L	141.4±56.486	58.583±2.483
UREA mmol/L	2.757±0.472	1.998±0.049*
CK U/L	442.267±38.585	439.733±26.190
α-HBDH U/L	28.633±1.962	32.383±3.144
HDL-C mmol/L	2.317±0.462	2.627±0.122
LDL-C mmol/L	0.410±0.076	0.287±0.034
LDH U/L	290.933±38.479	325.017±20.649
ALP U/L	2.467±0.674	3.533±0.314
T-Bil umol/L	1.160±0.096	1.308±0.062
Number of leukocytes (*103/UL)	5.327±0.280	3.837±0.686
Number of neutrophils (*103/UL)	1.353±0.246	0.937±0.229
Lymphocyte count (*103/UL)	3.670±0.156	2.640±0.432
Number of monocytes (*103/UL)	0.197±0.048	0.188±0.023
Number of eosinophils (*103/UL)	0.080±0.056	0.052±0.027
Number of basophils (*103/UL)	0.027±0.018	0.017±0.012
Percentage of neutrophils	25.150±3.512	22.780±2.326
Lymphocyte percentage	69.340±5.048	69.998±1.521
Monocyte percentage	3.623±0.667	5.710±1.173
Percentage of eosinophils (%)	1.443±0.931	1.092±0.568
Percentage of basophils (%)	0.447±0.294	0.422±0.259

Number of red blood cells (*106/UL)	7.123±0.138	7.485±0.262
Hemoglobin concentration (g/dl)	109.333±4.055	107.833±2.713
Hematocrit (%)	39.100±0.577	35.900±1.309
Mean corpuscular volume (Fl)	54.933±0.348	48.050±1.447
Mean hemoglobin content (pg)	15.200±0.404	14.450±0.339
Mean hemoglobin concentration (g/L)	277.000±6.245	301.500±7.261
RBC distribution width (%)	14.867±0.467	15.733±0.226
Platelet count (*103/UL)	532.667±42.881	536.333±66.231
Mean platelet volume (FL)	5.100±0.153	5.050±0.099

Data are means ± SEM, control (n=3); liquiritin (n=6); *P< 0.05 compared with control mice.

Supplementary Table 8：Body weight, organ index, blood chemistry and blood analysis in control or liquiritin-treated male mice by intraperitoneal injection.

	Control-male	Liquiritin-male	Liquiritin-male-recovery
Body weight, g	35.133±0.426	34.533±0.240	34.600±0.321
Brain index, %	1.243±0.038	1.307±0.024	1.320±0.046
Thyroid index, %	0.770±0.050	0.703±0.038**	0.787±0.048
Lungs index, %	0.537±0.012	0.570±0.040	0.540±0.035
Thymus index, %	0.150±0.010	0.220±0.010*	0.173±0.003
Heart index, %	0.420±0.015	0.387±0.012	0.443±0.013
Liver index, %	4.607±0.239	3.907±0.058	5.847±0.116*
Spleen index, %	0.267±0.027	0.417±0.035	0.343±0.018
Pancreas index, %	0.567±0.055	0.610±0.025	0.817±0.067
Kidney index, %	1.687±0.058	1.437±0.047	1.427±0.084
Testis index, %	0.683±0.009	0.617±0.029	0.663±0.009
Epididymis index, %	0.143±0.003	0.143±0.018	0.183±0.024
Stomach index, %	0.737±0.050	0.657±0.022	0.670±0.038
Bladder index, %	0.083±0.015	0.080±0.010	0.080±0.010
ALT U/L	131.833±27.310	45.100±5.856*	57.833±6.743
AST U/L	137.000±3.555	113.100±14.755	118.767±10.810
GLU-God mmol/L	3.753±0.387	3.680±0.996	9.350±0.356***
TC mmol/L	2.970±0.119	3.750±0.545	3.320±0.118
TG mmol/L	0.573±0.047	0.940±0.126	1.227±0.172*
TP g/L	71.800±19.310	60.100±3.600	55.133±0.617
ALB g/L	27.167±1.097	31.767±1.330	28.233±0.524
UA umol/L	74.967±4.101	106.567±16.136	53.900±1.504**
UREA mmol/L	2.217±0.119	1.933±0.027	2.237±0.182
CK U/L	335.200±72.660	481.600±53.306	517.767±25.695
α-HBDH U/L	39.900±5.900	34.433±9.089	30.067±4.784
HDL-C mmol/L	2.383±0.084	2.900±0.454	2.887±0.061**
LDL-C mmol/L	0.477±0.033	0.613±0.062	0.360±0.066
LDH U/L	443.900±48.916	433.600±112.348	314.100±54.673
ALP U/L	3.267±0.333	2.567±0.318	5.267±0.145**
T-Bil umol/L	1.533±0.194	1.310±0.140	1.760±0.068
Number of leukocytes(*103/UL)	6.020±0.652	5.700±0.495	7.513±0.615
Number of neutrophils(*103/UL)	1.600±0.186	2.907±0.257*	1.607±0.279
Lymphocyte count(*103/UL)	3.890±0.586	2.190±0.262	5.543±0.312
Number of monocytes(*103/UL)	0.337±0.041	0.547±0.166	0.020±0.006**
Number of eosinophils(*103/UL)	0.140±0.015	0.050±0.010**	0.340±0.080
Number of basophils(*103/UL)	0.047±0.020	0.003±0.003	0.003±0.003
Percentage of neutrophils	27.093±4.170	51.470±5.110*	21.063±2.056
Lymphocyte percentage	64.043±4.323	38.310±2.880**	74.157±2.703
Monocyte percentage	5.613±0.221	9.257±2.361	0.250±0.104***
Percentage of eosinophils(%)	2.383±0.377	0.863±0.127*	4.500±0.761

Percentage of basophils (%)	0.870±0.090	0.103±0.055**	0.027±0.018***
Number of red blood cells (*106/UL)	7.437±0.383	7.790±0.145	7.967±0.072
Hemoglobin concentration (g/dl)	104.000±4.041	114.000±1.000	111.667±3.180
Hematocrit (%)	36.533±1.081	38.767±1.444	35.367±0.581
Mean corpuscular volume (Fl)	49.300±1.909	49.767±0.949	44.367±0.437
Mean hemoglobin content (pg)	14.000±0.404	14.633±0.133	14.033±0.273
Mean hemoglobin concentration(g/L)	284.333±3.930	294.667±8.743	315.333±3.756**
RBC distribution width (%)	15.533±0.426	16.967±0.145*	16.567±0.780
Platelet count (*103/UL)	438.333±90.381	737.000±24.880*	771.333±33.418*
Mean platelet volume (FL)	5.333±0.120	4.933±0.176	4.700±0.153*

Data are means ± SEM, control (n=3); liquiritin (n=3); liquiritin-recovery (n=3); *P< 0.05 compared with control mice.

Supplementary Table 9：Body weight, organ index, blood chemistry and blood analysis in control or liquiritin-treated female mice by intraperitoneal injection.

	Control-female	Liquiritin-female	Liquiritin-female-recovery
Body weight, g	27.800±0.539	28.733±0.784	27.800±0.643
Brain index, %	1.597±0.064	1.533±0.038	1.670±0.040
Thyroid index, %	0.613±0.038	0.550±0.040	0.697±0.042
Lungs index, %	0.600±0.021	0.623±0.003	0.600±0.012
Thymus index, %	0.203±0.024	0.170±0.038	0.223±0.049
Heart index, %	0.433±0.009	0.407±0.018	0.443±0.024
Liver index, %	3.847±0.103	3.930±0.139	4.747±0.075**
Spleen index, %	0.370±0.040	0.473±0.043	0.457±0.035
Pancreas index, %	0.630±0.086	0.763±0.033	1.023±0.107*
Kidney index, %	1.137±0.038	1.160±0.059	1.260±0.062
Ovary index, %	0.107±0.003	0.117±0.017	0.120±0.010
Uterus index, %	0.550±0.125	0.460±0.031	0.727±0.111
Stomach index, %	0.853±0.029	0.827±0.027	0.780±0.025
Bladder index, %	0.070±0.000	0.070±0.000	0.070±0.000
ALT U/L	70.500±24.807	91.167±45.701	35.433±3.453
AST U/L	106.733±5.491	97.667±9.491	104.567±4.200
GLU-God mmol/L	4.027±0.499	4.707±0.624	8.417±0.205***
TC mmol/L	2.360±0.070	2.727±0.171	2.150±0.074
TG mmol/L	0.553±0.116	0.600±0.032	1.087±0.232
TP g/L	61.067±1.562	56.133±0.328*	52.300±2.031*
ALB g/L	32.400±1.457	32.967±0.291	27.933±1.068
UA umol/L	100.867±9.870	144.033±27.929	51.200±3.772**
UREA mmol/L	2.300±0.154	1.967±0.064	2.130±0.127
CK U/L	256.967±69.036	226.933±30.633	446.233±103.245
α-HBDH U/L	36.033±2.862	25.333±2.946	27.933±1.068
HDL-C mmol/L	2.147±0.192	2.080±0.200	1.840±0.000
LDL-C mmol/L	0.450±0.026	0.440±0.025	0.323±0.038
LDH U/L	376.767±31.053	315.467±42.721	250.400±53.029
ALP U/L	2.333±0.788	2.667±0.120	13.667±2.206**
T-Bil umol/L	1.377±0.068	0.947±0.175	1.653±0.136
Number of leukocytes (*103/UL)	4.767±1.188	5.107±0.775	6.267±1.109
Number of neutrophils(*103/UL)	0.920±0.388	2.013±0.475	0.970±0.142
Lymphocyte count (*103/UL)	3.603±0.814	2.380±0.194	4.873±0.943
Number of monocytes (*103/UL)	0.227±0.015	0.637±0.182	0.013±0.007**
Number of eosinophils(*103/UL)	0.0133±0.007	0.070±0.035	0.403±0.083
Number of basophils (*103/UL)	NA	0.013±0.009	0.003±0.003
Percentage of neutrophils	16.943±5.317	38.483±3.150*	15.790±2.024
Lymphocyte percentage	77.073±3.560	47.507±3.438**	77.363±1.396
Monocyte percentage	5.697±1.983	12.290±2.581	0.263±0.104
Percentage of eosinophils (%)	0.250±0.098	1.457±0.812	6.473±1.175**

Percentage of basophils (%)	0.033±0.020	0.263±0.166	0.100±0.075
Number of red blood cells (*106/UL)	6.993±0.515	7.493±0.074	7.643±0.038
Hemoglobin concentration (g/dl)	98.000±11.930	113.667±0.333	107.000±2.082
Hematocrit (%)	33.067±4.103	38.667±0.437	34.867±1.133
Mean corpuscular volume (Fl)	46.900±2.916	51.633±1.081	45.634±1.485
Mean hemoglobin content (pg)	13.933±0.845	15.167±0.133	13.967±0.318
Mean hemoglobin concentration (g/L)	296.667±2.848	294.000±4.163	307.000±7.234
RBC distribution width (%)	15.500±0.379	16.467±0.145	16.333±0.233
Platelet count (*103/UL)	612.667±42.049	613.000±48.952	597.000±25.813
Mean platelet volume (FL)	4.733±0.233	4.833±0.176	4.667±0.145

Data are means ± SEM, control (n=3); liquiritin (n=3); liquiritin-recovery (n=3); *P< 0.05 compared with control mice.